

CFD Case Study of the JPMorgan Chase Tower

Khalid Boulbrachene, Mahmoud Ammar, Rahul Krishna*

Abstract

This report aims to explain the literature review, work flow, and results of a group project done in the winter semester 2019 at the Chair of Structural Analysis at the Technical University of Munich supervised by Philipp Bucher. The main task was to set-up and run CFD analysis on the JPMorgan Chase Tower according to the Eurocode. In this present work, the pre-processing was done using GiD, the analysis was performed using Kratos Multiphysics, and the post-processing using ParaView.

Keywords: Computational Fluid Dynamics, Structural Wind Engineering, Kratos Multiphysics.

Introduction

Computational fluid dynamics (CFD) is the study implementation of the physics behind how a fluid flows, in which it is based on Navier Stokes Equations that explain how velocity, pressure, temperature, and density of a fluid are linked to each other.

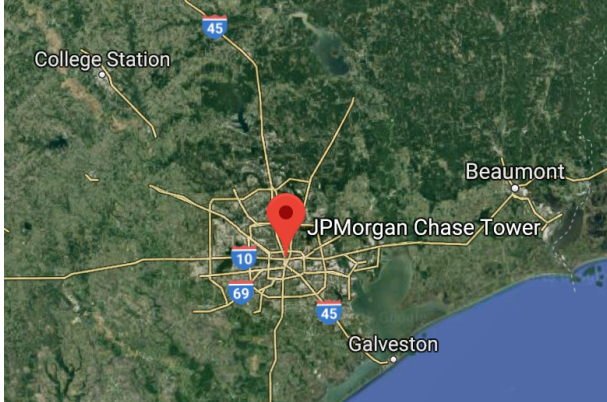
Usually, experimental studies that involve wind tunnel tests are too expensive to perform and complicated to apply, but their output is limited to where the sensors are put. Here comes the use of numerical modelling which is cheaper and it gives better data regarding the velocity and pressure fields of the whole computational domain. This does imply that wind tunnel testing can be sacrificed for CFD, but using CFD to run analysis during the design process, then validating the results using wind tunnel testing would be the ideal case [2].

This report is about the CFD analysis of the JPMorgan Chase Tower in which the wind load on the building is studied. Furthermore, some geometrical modifications are done to see the difference in the vortex shedding. Most of the calculations are in accordance to the Eurocode.

1 General Information

The JPMorgan Chase Tower is located in Houston, a city in the state of Texas of the United States of America [Figure 1a]. The construction started in 1978 and was completed in 1982, and it is ranked the 121 tallest building in the world. The building's height is 305.4 meters, and it has 75 floors above the ground. The core is composed of reinforced concrete, and the columns and floor spanning are composed of steel [1].

* Technical University of Munich, Chair of Structural Analysis



(a) Satellite image



(b) 3D image of the building's surrounding

Figure 1: Location map (source: www.maps.google.com)

The building was firstly designed to have 80 floors, but the height of the tower was decreased by the Federal Aviation Administration which announced that any building higher than 75 floors in downtown Houston will be a risk on air navigation. Moreover, the building has 6 sides, 5 of them have exterior windows [1].

2 Wind Climate and Exposure

2.1 Terrain Category

According the Eurocode EN 1991-1-4, there are 5 main terrain categories which are explained in Table 1, and the selection of the terrain category is important for finding the gust wind speed profile.

0	Sea or coastal area exposed to the open sea
I	Lake or flat and horizontal area with negligible vegetation and without obstacles
II	Area with vegetation such as grass and isolated obstacles with separations of at least 20 obstacle heights
III	Area with regular cover of vegetation or buildings or with isolated obstacles with separations of maximum 20 obstacle heights
VI	Area in which at least 15% of the surface is covered with buildings and their average height exceeds 15m

Table 1: Different terrain categories explained [5]

To select the terrain category for the JPMorgan Chase Tower, the surrounding of the building has to be observed. In Figure 1b, it is clear there are buildings with a height that exceeds 15 m from all directions, so terrain category VI is selected for all directions.

In reality, a wind rose of the dominant wind direction has to be used to find the angle of the dominant wind direction as shown in Figure 2 which shows that the dominant wind direction, from 1st of June, 1969 till 22nd of February 2019, is few positive degrees away from south, then the surrounding of this direction should be checked to decide on the category type.

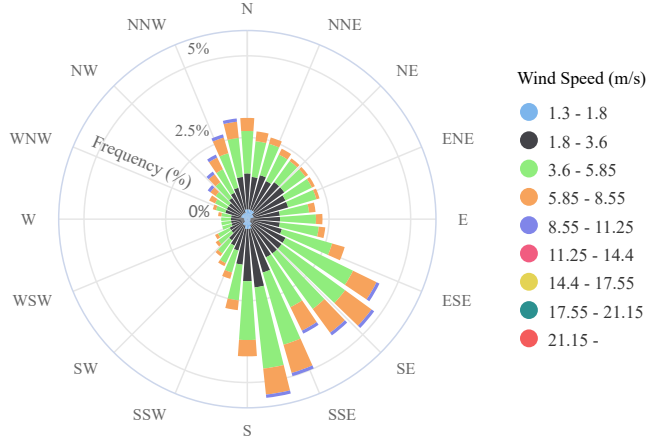


Figure 2: Wind rose (source: www.mrcc.illinois.edu)

2.2 Atmospheric Boundary Layer

The atmospheric boundary layer (ABL) is located at the lowest region of the atmosphere in which the structures on the ground will affect it. It will be zero on the ground because of the no slip condition and it will increase with the height.

In order to find the velocity profile, the gust wind speed has to be calculated. To do so, the wind speed data for a period over 72 years was taken from the National Oceanic and Atmospheric Administration database [4], and the Gumbel method is used to find the extreme wind estimation.

2.2.1 Gumbel Method

This method is based on taking the largest wind speed for each year that is recorded. First, the wind speed is ranked from the smallest to the largest (1 to N; N is the number of years recorded). Second, each gust wind speed is given a probability of non-exceedence [Equation 1] such that m is the rank for each gust wind speed [3].

$$P = \frac{m}{N+1} \quad (1)$$

Third, the reduced variate is calculated using Equation 2 [3].

$$y = -\ln(-\ln(P)) \quad (2)$$

Fourth, the variation of the reduced variate y as a function of the gust wind speed is plotted including a curve fitting as in Figure 3.

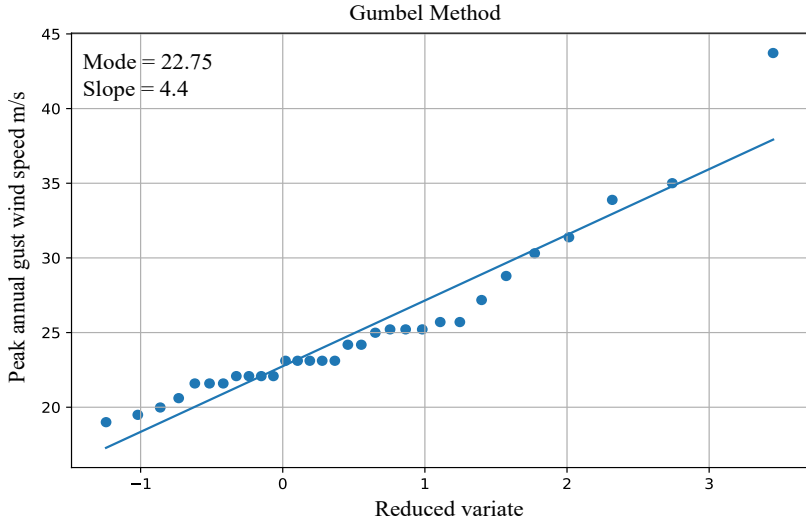


Figure 3: Curve fitting of the gust wind speed

Finally, the mode of distribution and the scale factor (slope) of the curve fitting are used to find the Gumbel predicted gust wind speed for 50 years return period (i.e. happens one time every 50 years) to have an expected frequency equivalent to 2% [Equation 3]. It is chosen to be 50 years because that's the most common choice [3].

$$U_{gust-50 \text{ years}} = mode + slope \left[-\ln \left(-\ln \left(1 - \frac{1}{50} \right) \right) \right] \quad (3)$$

2.2.2 Velocity profile

Following the steps in Section 2.2.1, the gust wind speed is found to be 39.91 m/s. First, the mean wind speed has to be found, which can be done using Equation 4 knowing that the wind load factor γ_w is 1.4 which is used as a factor to convert from gust to mean wind speed [5].

$$U_{mean} = \frac{U_{gust-50/\text{years}}}{\gamma_w} \quad (4)$$

According the Eurocode EN 1991-1-4, the gust and mean velocity profiles for terrain category IV [Section 2.1] can be found using Equations 5a and 5b, respectively [5].

$$U_{gust}(z) = z_{0,gust} * U_{mean} \left(\frac{z}{10} \right)^{\alpha_{gust}} \quad (5a)$$

$$U_{mean}(z) = z_{0,mean} * U_{mean} \left(\frac{z}{10} \right)^{\alpha_{mean}} \quad (5b)$$

For the gust velocity profile, the roughness $z_{0,gust}$ is 1.05 m, and profile exponent α_{gust} is 0.2. On the other hand, for the mean velocity profile, $z_{0,mean}$ is 0.56 m, and α_{mean} is 0.3. substituting all the coefficients with the U_{gust} will give the velocity profiles in Figure 4 [5].

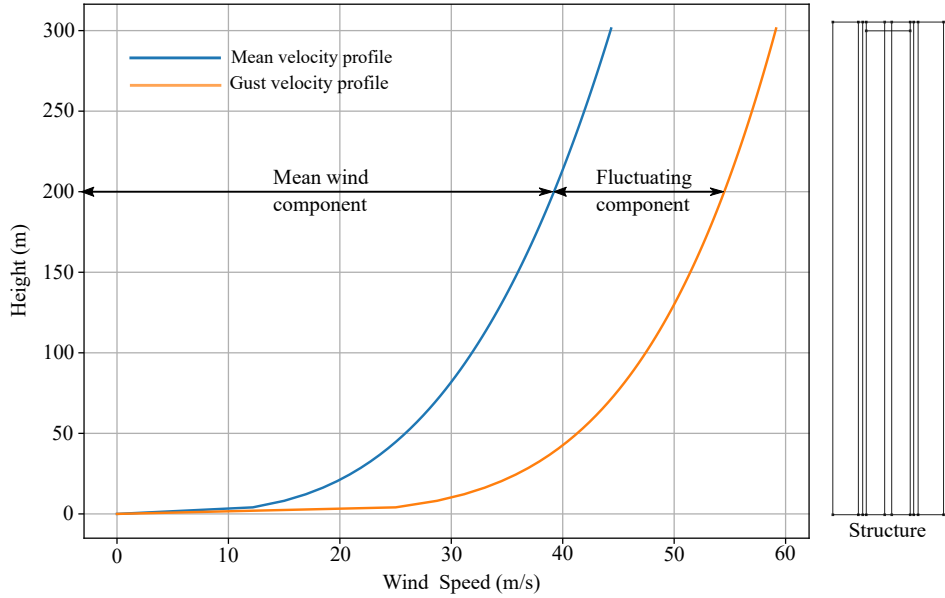


Figure 4: Mean and gust velocity profiles along the structure

The gust wind speed profile is the combination of both, the mean wind component and fluctuating component. The gust wind speed profile will be used in the analysis which will be discussed in the following chapters.

3 Aerodynamic Preliminary Analysis

3.1 Base Static Shear and Moment

The static shear force at the base T_s is equivalent to the total static drag forces along the height of the building as shown in Equation 6. Where H is the height of the building, $P(z)$ is the pressure distribution along the height, ρ is the density of the air assumed to be $1.225 \frac{kg}{m^3}$, C_D is the drag coefficient, and A is the orthogonal surface to the velocity field.

$$T_s = \int_0^H P(z) b dz \approx \sum_{i=1}^{\#sec} \frac{1}{2} \rho u_i(z)^2 C_D A_i \quad (6)$$

One can simplify the integral as the summation over building sections. First, the building is vertically divided into equal sections and the drag force is computed for each section considering its respective area, height, and averaged gust wind speed. Then, the base static shear force is obtained by summing all contributions. Eventually, the drag coefficient reflecting the shape of the cross section is obtained from the Eurocode. The building's cross section is simplified and considered to be a rectangle of width $b=68.96m$ and a depth of $d=57.56$. Therefore, using Figure 5 the aspect ratio $d/b=1.2$ which by logarithmic interpolation corresponds to a C_D value of 2.2.

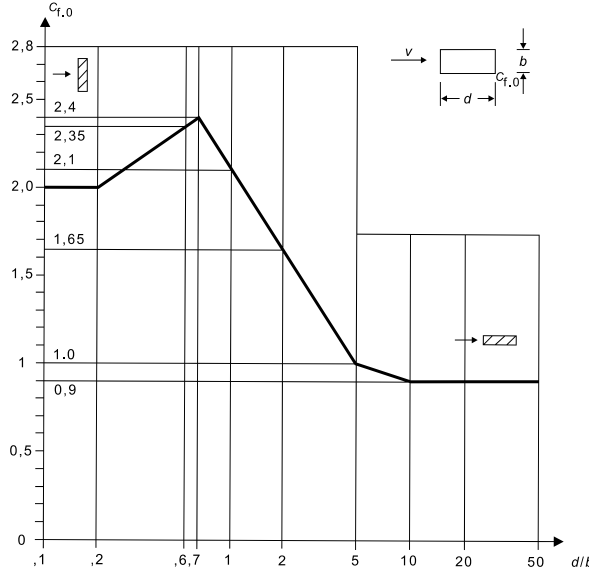


Figure 5: Drag coefficient for sharp rectangular cross-section [5]

Similarly, the base static bending moment M_s is found by the multiplication of the drag of each section $F_{D,i}$ by the lever arm z_i , namely, from the base to the section's middle point.

$$M_s = \int_0^H F_D(z) dz \approx \sum_{i=1}^{\#sec} F_{D,i} z_i \quad (7)$$

Drag force and moment distribution along the height of the building are showed in the Figure 6. The calculated base shear force and moment are $T_S = 139.83$ MN and $M_S = 24911.18$ MNm , respectively.

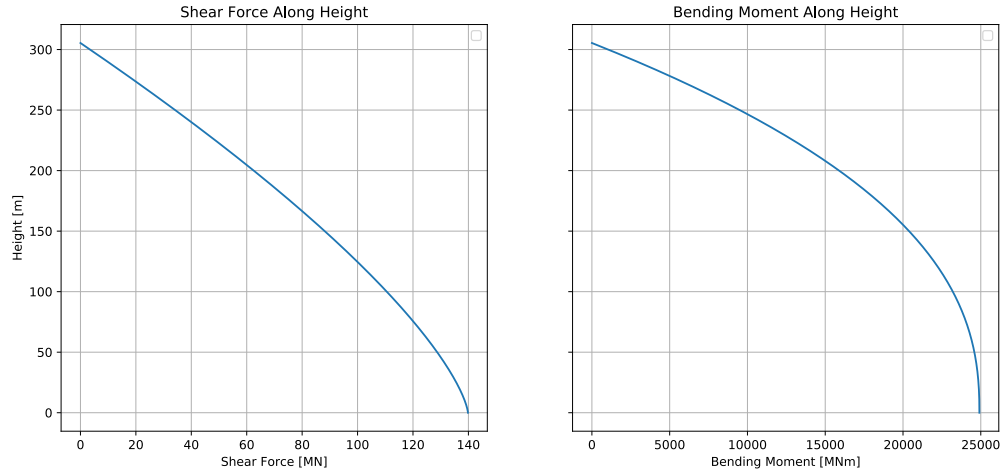


Figure 6: Shear and moment along the height

3.2 Dynamic Shear and Moment

Using the values calculated in Appendix 6.1, the size and dynamic factors are calculated to be:

$$C_s = 0.83$$

$$C_d = 1.463$$

Both, the dynamic shear force T_{Dyn} and the dynamic bending moment M_{Dyn} at the base of the building are computed using Equations 13a and 13b, respectively. The profiles of the dynamic shear force and bending moment along the height of the building are similar to the ones obtained for the static case but scaled by the multiplication of structural factors C_s and C_d . The obtained results are:

$$T_s = 167.8 \text{ MN}$$

$$M_s = 29894.1 \text{ MNm}$$

3.3 Natural Frequency Analysis

Given the fact that the building under this study has a considerable height, the frequency analysis becomes more important, to know the first three natural frequencies of the structure. These frequencies are a function of the mass, stiffness and damping of the system, and can be obtained analytically by solving an eigen-value problem. Due to the complexity of the problem an empirical formula provided in Equation 8, based on the height of the structure was used [5]. To validate the result, a finite element frequency analysis was carried out in a FE solver, SolidWorks.

$$n_{1,x} = \frac{46}{H} \quad (8)$$

Figures 7a, 7b, and 7c show building mode-shapes corresponding to different eigen-frequencies. It can be observed that the first three mode-shapes are dominated by bending, which is similar to that of a cantilever beam. The first eigen-frequency obtained by the frequency analysis from SolidWorks matches to a good extent with that calculated from the empirical formula.

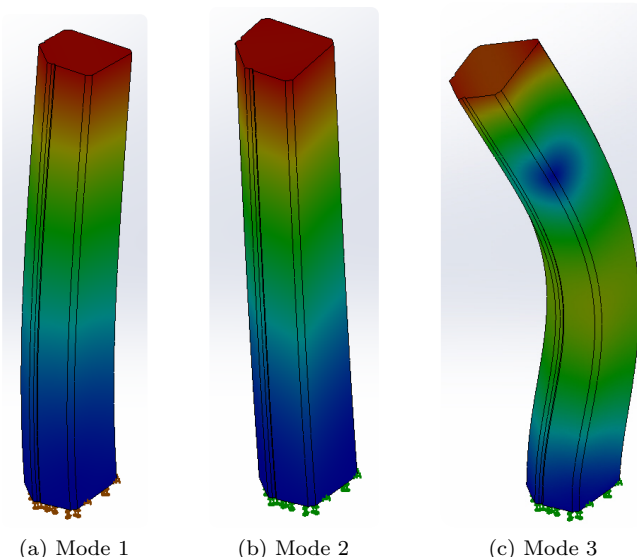


Figure 7: First 3 mode shapes

3.4 Vortex Shedding

Vortex shedding takes place when vortices are shed alternately from opposite sides of the building, which gives a rise to fluctuating load perpendicular to flow direction. When vortices shed from the sides of the building periodically and their frequency matches the building's resonance frequency, they are said to be critical as they induce cross-flow vibrations. In order to compute this frequency, Strouhal number (St) is used. Strouhal number is a dimensionless number describing oscillating flow mechanisms, and it is defined in Equation 9

$$St = \frac{f L}{U} \quad (9)$$

Where f is the frequency of the vortex-shedding, L is the characteristic length and U is the characteristic flow velocity. Figure 8 illustrates experimental results of Strouhal number found for different rectangular aspect ratios.

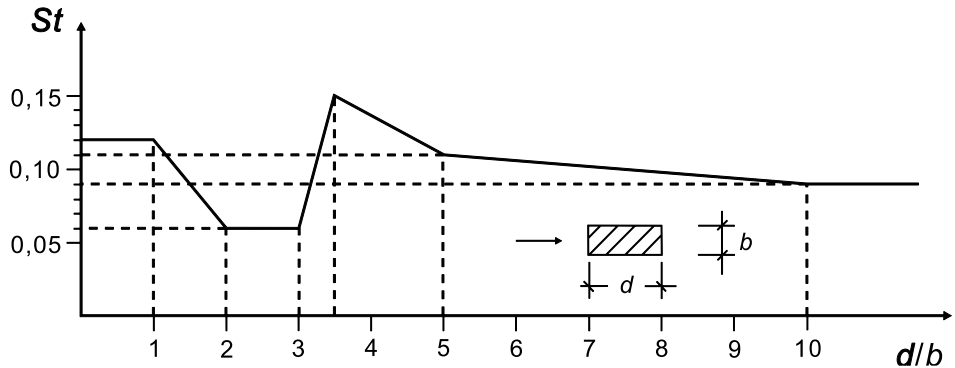


Figure 8: Strouhal number according to the aspect ratio [5]

To find an estimate of the Strouhal number, Figure 8 is used. The simplified cross-section of the JPMorgan Chase Tower is a rectangle with an aspect ratio of $\frac{d}{b} = \frac{57.56}{68.96} = 0.834$ which corresponds to a Strouhal number value of 0.12 [5]. The width of the building is taken to be the characteristic length, therefore, $L = 68.96\text{m}$. Finally, flow velocity is assumed to be equal to the mean wind speed, which is equal to 39.91 m/s based on section 2.2.2.

Substituting the values to Equation 9, the vortex-shedding frequency $f_{vs} = 0.069 \text{ Hz}$. Using Equation 8, $n_{1,x} = 0.15 \text{ Hz}$ which does not match f_{vs} .

On the other hand, the critical wind velocity of mode i which is defined as the velocity at which the vortex shedding frequency equals the natural frequency of the building is computed using Equation 10 which gives the value 86.2 m/s.

$$U_{crit,i} = \frac{b n_{i,x}}{St} \quad (10)$$

For safety measures, the critical wind velocity is supposed to be greater than 1.25 times the flow velocity [Equation 11] [5]. Since that the criteria is fulfilled, one can claim that no structural vibrations will be induced due to vortex shedding.

$$1.25 U < U_{crit} \quad (11)$$

4 Pre-processing

4.1 Geometric modeling

The dimensions of the computational domain [Figure 9] are chosen to be 3 times the building's height for both, the length from the inlet to the structure and distance to the wall of the domain, and 6 times from the structure to the outlet. The clearance from the inlet is big to give time for the wind to fluctuates before it reaches the structure, and it is even bigger after the structure to capture the vortex shedding phenomena. On the other hand, the sides of the building to the wall and height above it are taken to be 1.5 times the height of the structure from both sides which is to guarantee a no-slip condition.

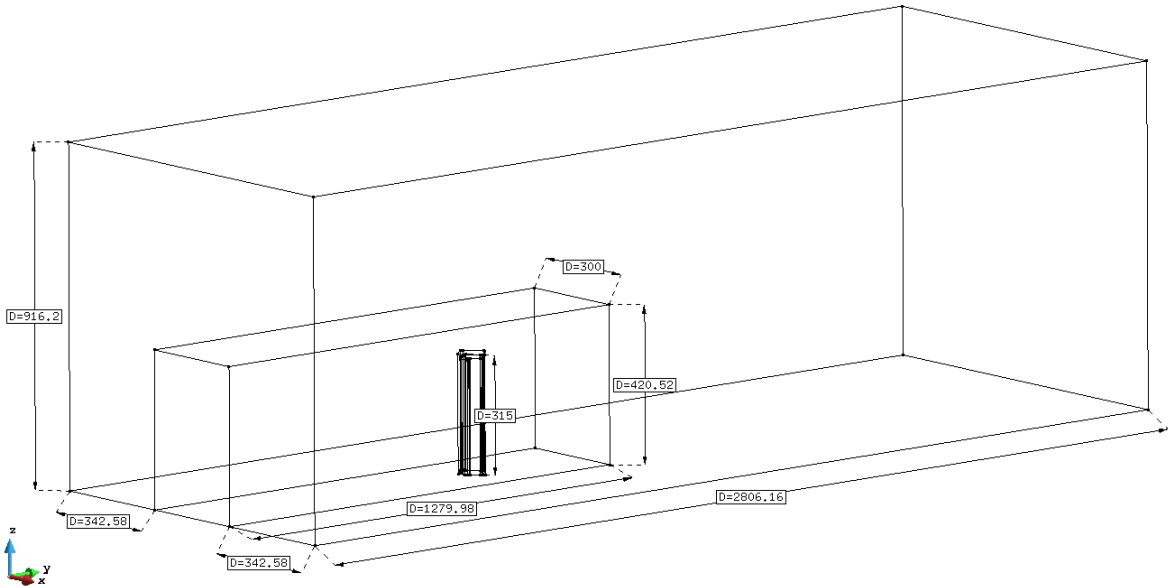


Figure 9: Building bounding box, middle bounding box, and main computational domain

There are 3 regions inside the computational domain. First, the building bounding box [Figure 10b] which is added to have a finer mesh inside to ensure a proper capturing of the physics around the structure. Second, 2 more bounding boxes as shown in Figure 10a. The use of these 2 bounding boxes is to ensure a smooth transition of the mesh size from the building bounding box to the main computational domain. Also, these 2 internal bounding boxes start from the inlet to guarantee the survival of the fluctuations of the wind speed profile.

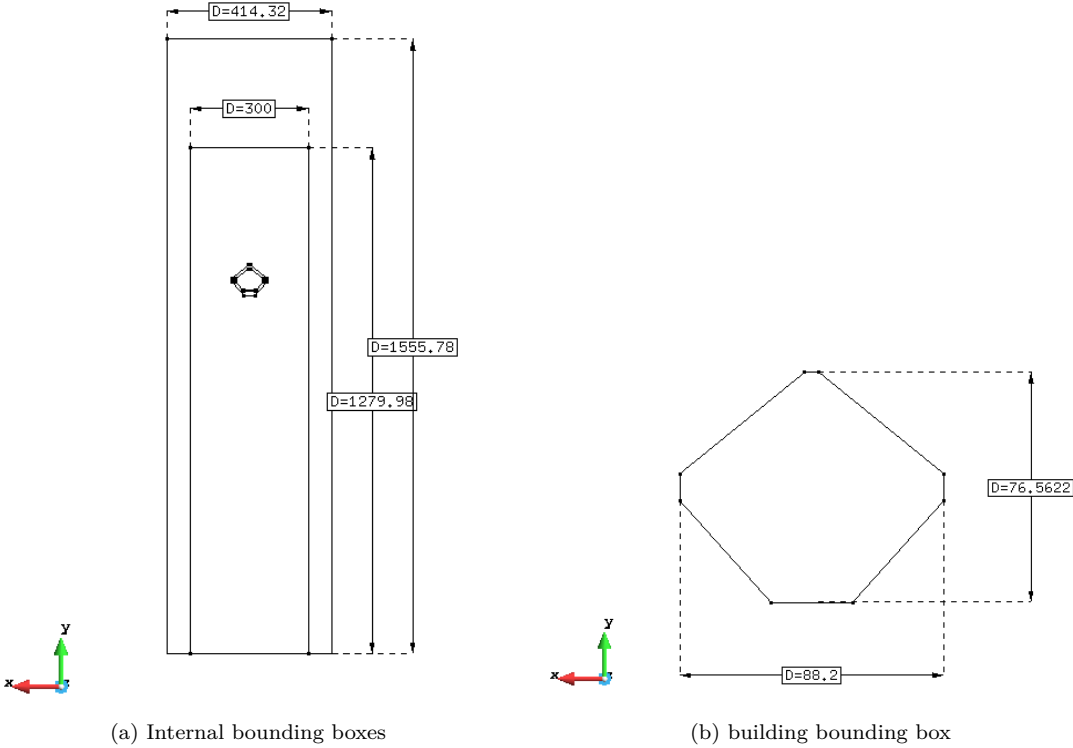


Figure 10: Bounding boxes for meshing

4.2 Meshing

The unstructured mesh is generated on the surfaces using the RFast algorithm in GiD. In addition, the sizes for the mesh generation are chosen as illustrated in Figure 11.

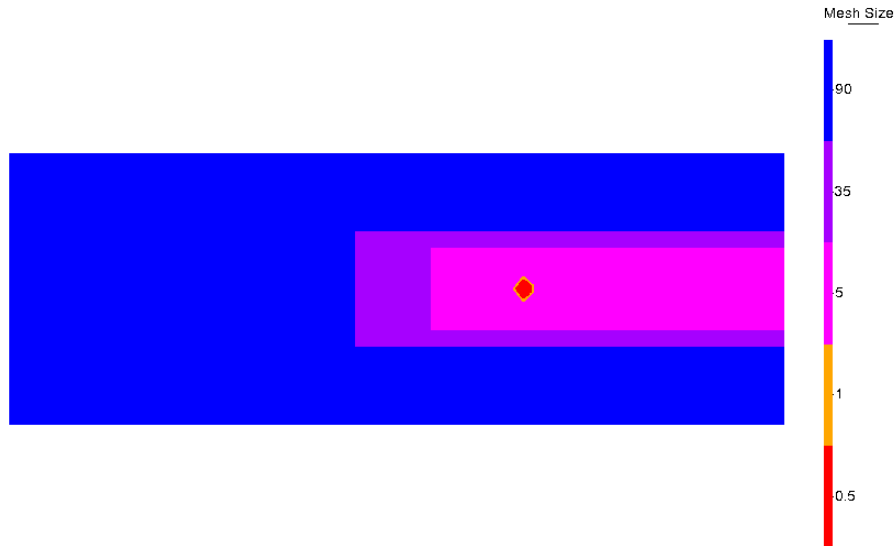


Figure 11: Assigned sizes on the surfaces

The mesh is generated with a size transition equal to 0.3 [Figure 12a]. The total number of elements is approximately 4.4 million concentrated mostly around the structure and the first rectangular bounding

box around it. Figure 12b shows how the mesh is too fine around the structure compared to the biggest element size in Figure 12a.

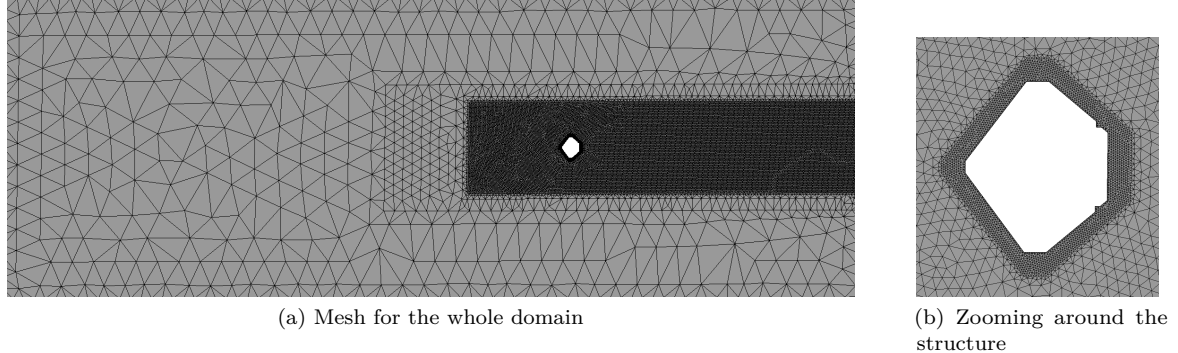


Figure 12: Bounding boxes for meshing

4.3 Numerical set-up

The CFD solver in Kratos Multiphysics is used to solve the unsteady Navier-Stokes equations for incompressible flow. The turbulence model used is the Variational Multiscale (VMS) Method which is the finite element equivalent to the finite volume Large Eddy Simulation (LES) turbulence model.

VMS is based on the concept of separation of the variables into small and large scales such that this separation is directly connected to the spatial discretization as represented in Figure 13. The large scales consist of what can be described using the finite element interpolation, but small scales consist of what cannot be reproduced because of the restrictions enforced by the discrete interpolation [2].

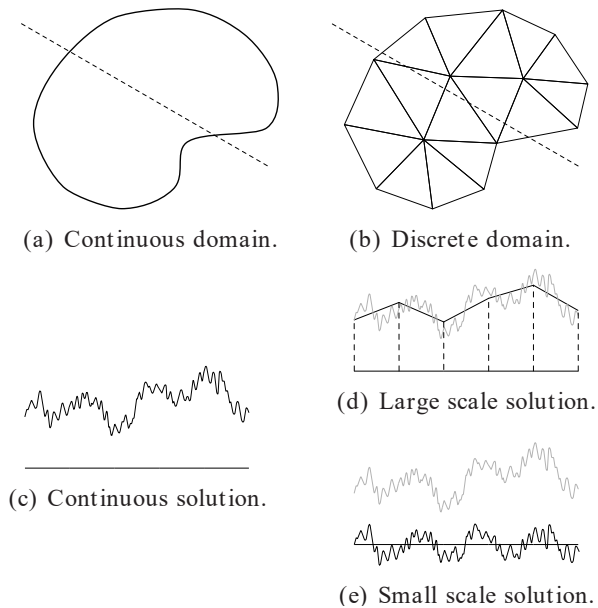


Figure 13: Scale separation [2]

To choose the proper time step size Δt for the simulation, the largest tolerated Δt can be calculated using Equation 12 which will give in this case approximately $\Delta t = 0.02$. The simulation time is 100 seconds,

therefore it will have in total 5000 iterations. In addition, the wind direction will be facing the building's front side towards the south.

$$\Delta t = CFL \frac{\Delta x}{u F} \quad (12)$$

5 Post-processing

5.1 Original Design of the Structure

5.1.1 Results visualization

After running the simulation which took almost 4 days to finish, the post-processing is done using Paraview, and all screen-shots are taken at $t = 100$ seconds. Figure 14 shows the longitudinal cut cutting the structure symmetrically. It is obvious that the velocity profile increases as the height increases reaching 110 m/s at the wall of the computational domain, the no-slip condition can be observed on the ground since the velocity is zero, and the stagnation point is all over the center line of the front side of the structure. Also, the separation point is on the top of the structure, and the velocity above it is too high because of the Bernoulli effect.

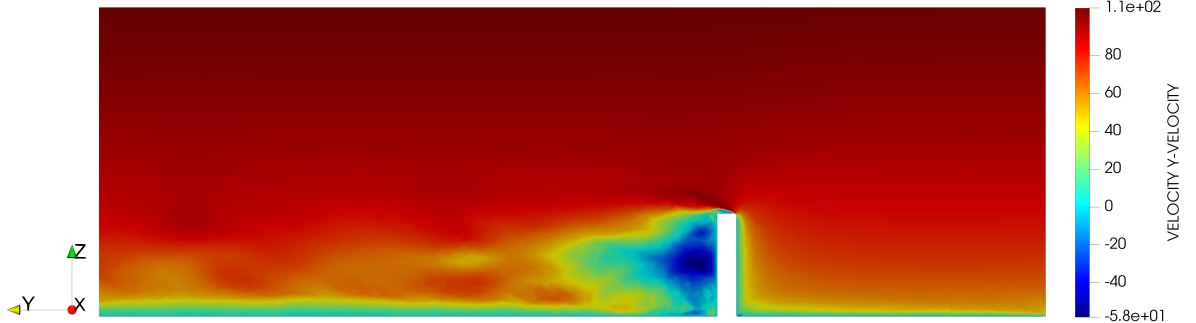


Figure 14: Longitudinal cross-section

In Figure 15, the vortices are shedding periodically in the wake region after the flow separation that occurs from the sides of the buildings. There is a direct relation between the grid size around the structure and proper capturing of the vortex shedding phenomena which is why the mesh is fine in that region.

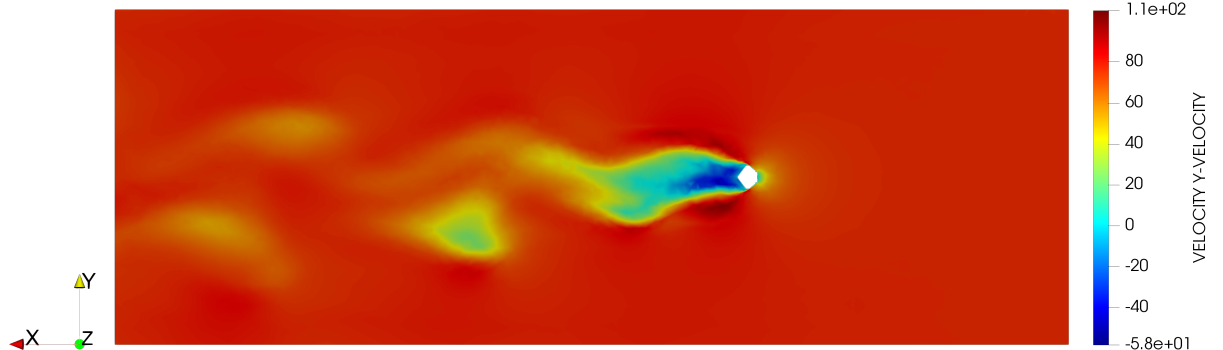


Figure 15: Horizontal cross-section

The flow separation can be noticed more in Figure 16 such that shape has two small curvatures which is caused from the inclination that occurs in the last few floors of the building.

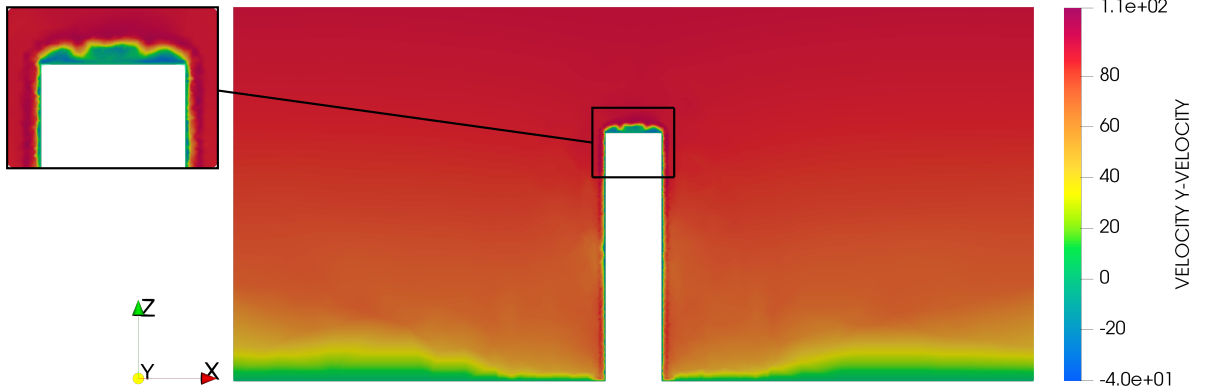


Figure 16: Cross-wind section

Figure 17 shows the pressure distribution along the structure. It is observed that the pressure along the front side of the structure increases from the bottom to the top. On the sides of the building after separation, the pressure values become negative because of the suction pressure created behind the building due to the flow separation. Further analysis regarding the C_p along the major sides of the building will be discussed in the following section.

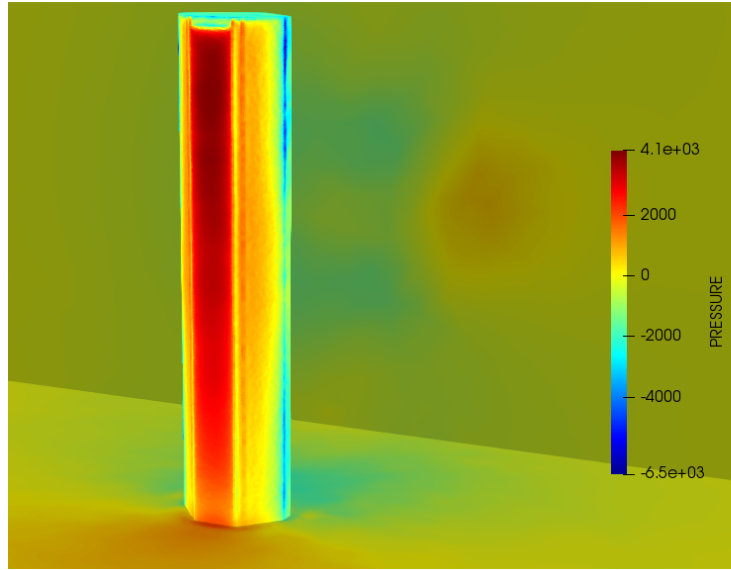


Figure 17: Pressure distribution

The plot is known as Surface LIC which is an interesting plug-in in ParaView. It is a vector visualization technique similar to visualizing streamlines. The difference being that here the streamlines are plotted for the entirety of the flow. The topology of the vector field becomes much clearer. The top view in the LIC plot in Figure 18 clearly shows the vortex shedding region, where the eddies grow in size in the wake region leading to a Karman-vortex-street.

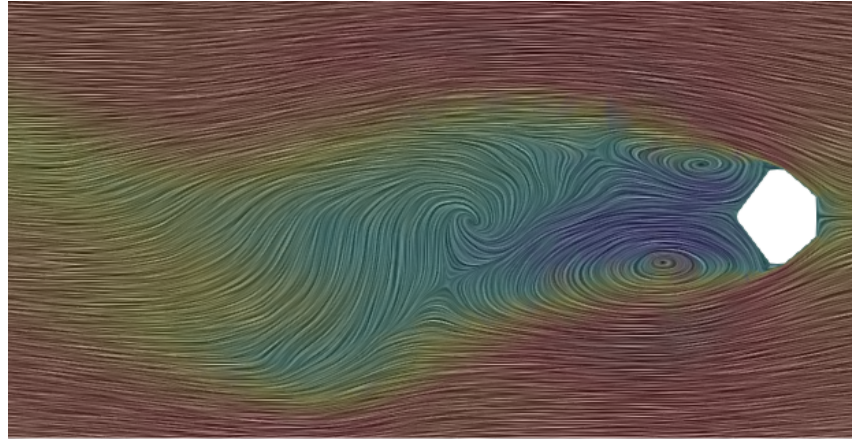


Figure 18: Streamlines - Horizontal cross-section

As it can be seen in the surface LIC plot [Figure 19], a huge recirculation zone behind the building is present in the wake of the flow. A very small circulation can also be observed on the bottom of the building facing the upstream flow. Also, the flow separation point can be identified from this plot.

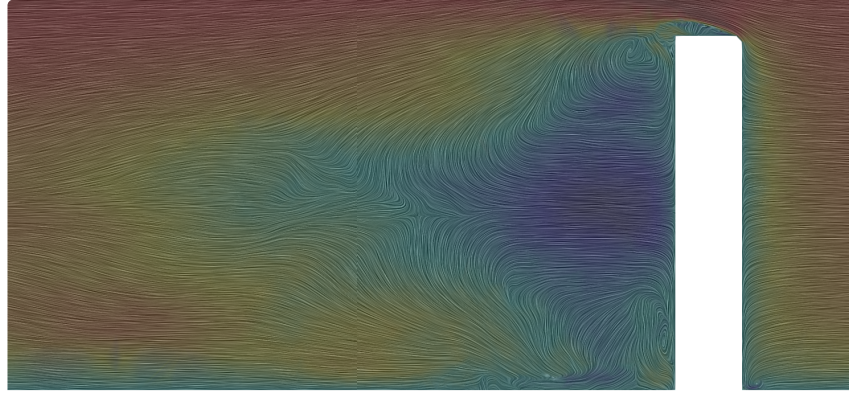


Figure 19: Streamlines - Longitudinal cross-section

5.1.2 Pressure coefficient (C_p)

A reference point was located at half of the distance between inlet and the building. The height of the point was chosen at two third of the building's height. Line results were then extracted at several defined lines on the building in order to generate the C_p values in which are shown in Figures 20a, 20b, and 20c.

It can be clearly seen that on the first defined line [Figure 20a], which was directly perpendicular to the downstream direction the C_p value varies between 0 and 1. It is very close to 1 exactly in the center which is the stagnation point.

In the line plots for the points on the other faces [Figures 20b and 20c], it is observed that the C_p value becomes negative, indicating that the velocity is increased by the potential energy of the free stream static pressure, being converted into kinetic energy. In addition it also indicates the presence of a suction pressure where the pressure at the structure is less than the ambient pressure, which initiates flow separation.

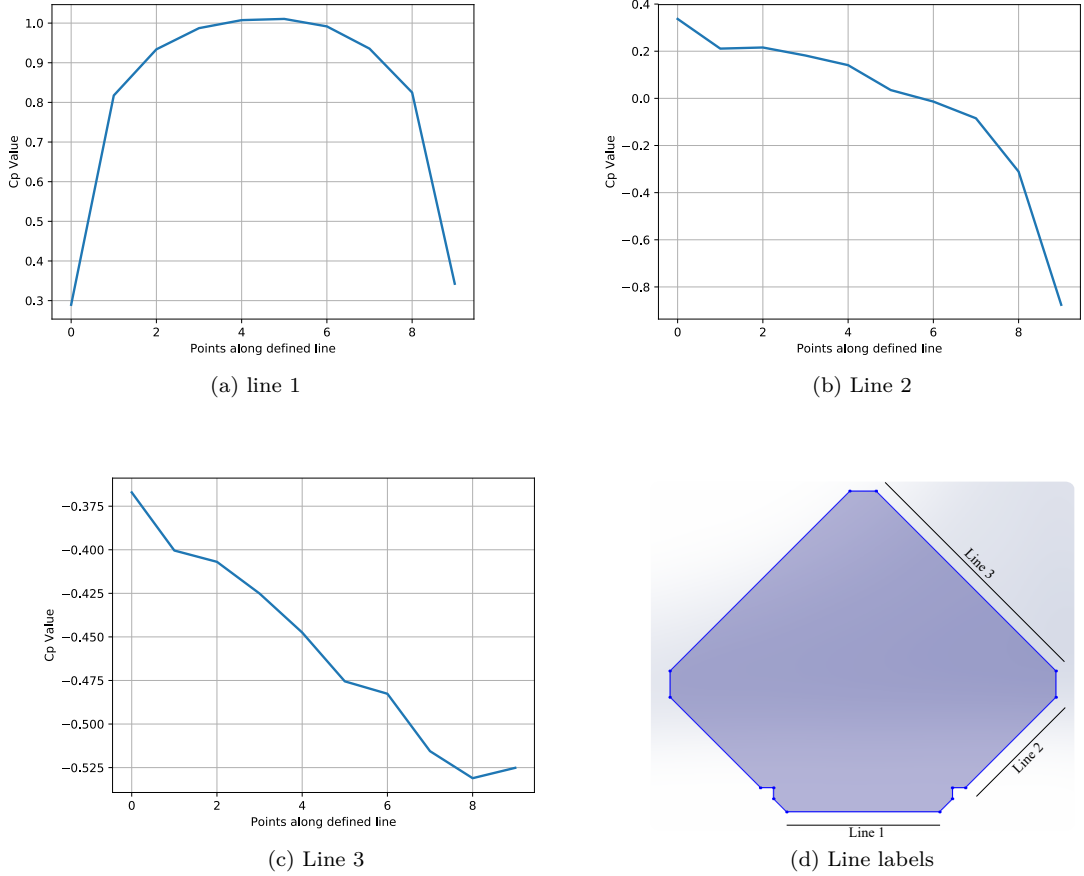


Figure 20: Cross-sections for both buildings

5.1.3 CFD base static shear and moment

The static and dynamic shear and moment computations were based on numerous simplifications and thus, the values cannot be taken as exact. But they rather serve as a preliminary result for the study. As getting analytical results for a high-rise building is not possible, so either numerical simulations or wind tunnel experiments have to be performed.

A quantitative analysis of the simulated base forces in comparison with the results obtained from the Eurocode in Sections 3.1 and 3.2 give an impression of the safety margins considered in the Eurocode. In the simulations, the logarithmic wind speed profile based on the mean wind speed produced significantly lower static shear and moment at the base, compared to the simplified values obtained considering the Eurocode. For the shear these data differ by 54%, and on the other hand for the moments the difference is 49%. This could be explained by the fact that the Eurocode is more on the safer side.

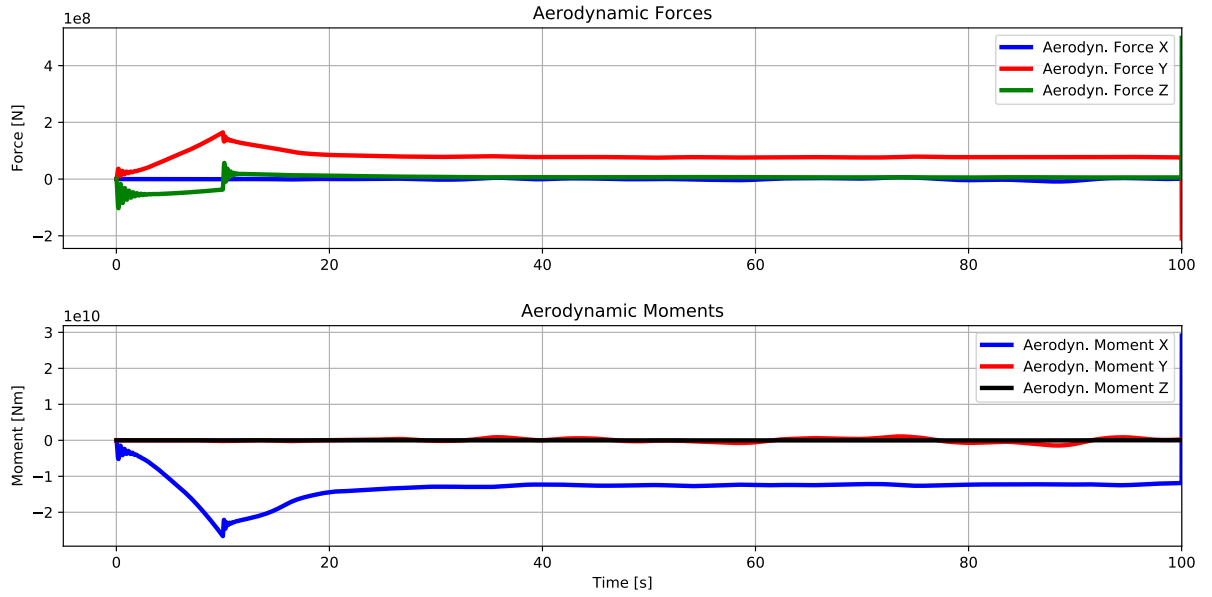


Figure 21: Longitudinal cross-section

5.2 Modified Design

In order to show how the buildings is designed to reduce the wake region, the cross-section of the building was modified to remove the small corners around the buildings [Figure 22a] and sharp edges were added as shown in Figure 22b. All the screen-shots are taken at $t = 100$ seconds.

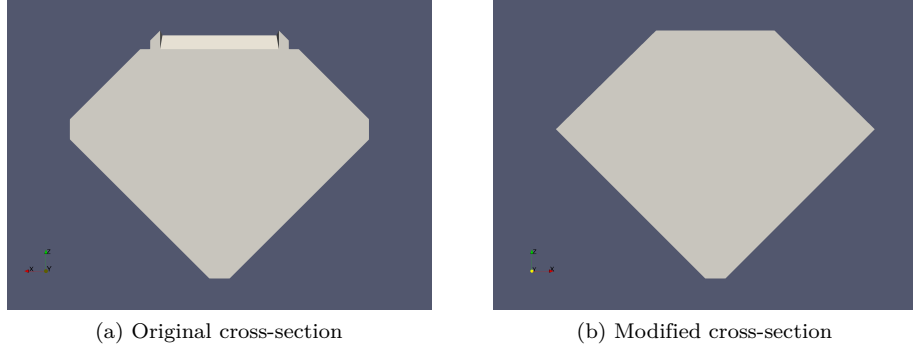


Figure 22: Cross-sections for both buildings

Figure 24 shows how the modification explained in Figure 22 affected the wake region such that the recirculation area became much more wider than in Figure 14. Also, the separation at the top of the building is contributing more to the wake region than with the chamfered edge.

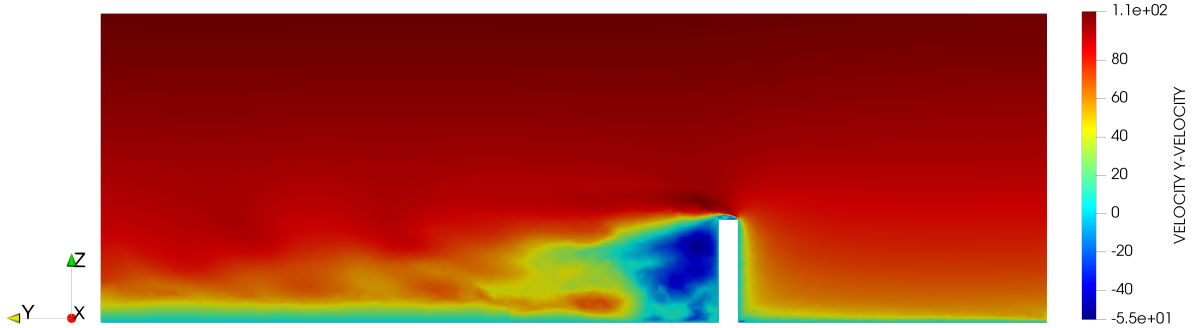


Figure 23: Longitudinal cross-section

In addition to that, the horizontal cross-section of the modified design in Figure 24 shows more clearly the wider wake region compared to Figure 16, and how the high velocity density is larger at the separation region. This is because the separation happens more violently when the small corners and the chamfered edges are removed from both sides followed by adding sharp edges.

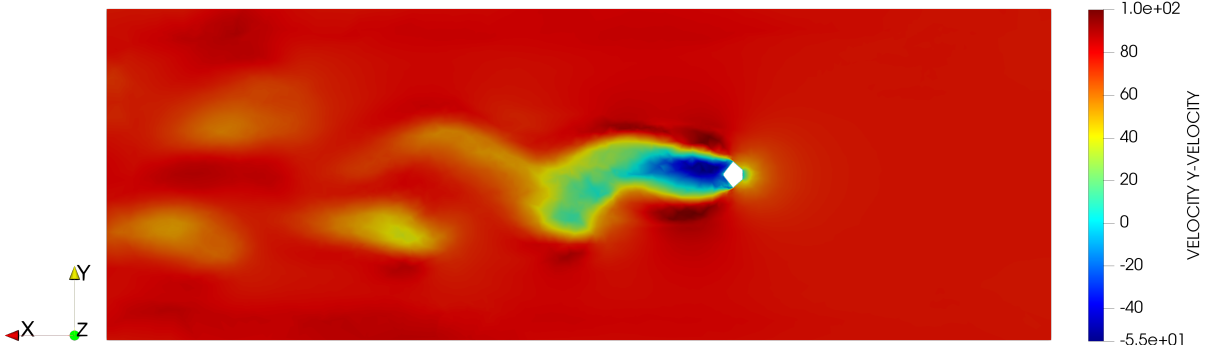


Figure 24: Horizontal cross-section

Conclusion

For the high-rise structure of this project, JPMorgan Chase Tower (Houston), the height was considerable and a wind load analysis is not only desirable but is a very important step in the design process. As seen in the results, the velocity magnitudes at this height can be significantly higher and a detailed wind load analysis is important.

Although the velocity profile across the building was significant, the building's design was made to reduce the size of the wake region. To study this phenomena, minor changes were performed in the cross-section of the building e.g. introducing sharp corners, in order to compare the simulation results and understand the effect of these simple changes. The simulation results for the model with the sharp corners and edges clearly showed that the flow separation took place earlier than compared with the actual model. Also, the wake region behind the building became adverse and grew in size. This study led us to understand the importance of these small features for reducing the wind load.

A complete FSI study for this problem is complex, and the project was aimed mainly on the CFD analysis. As a future outlook, coupling can be implemented in order to get more accurate representation of the phenomenon.

References

- [1] The Skyscraper Center.
JPMorgan Chase Tower.
URL: <http://www.skyscrapercenter.com/building/jpmorgan-chase-tower/472>.
- [2] Jordi Cotela Dalmau.
“Applications of turbulence modeling in civil engineering”.
PhD thesis. Universitat Politècnica de Catalunya.
- [3] John D. Holmes.
Wind Loading of Structures.
Spon Press, 2004.
- [4] National Oceanic and Atmospheric Administration.
URL: <http://www.noaa.gov>.
- [5] *EN 1991-1-4 Eurocode 1: Actions on structures - Part 1-4: General actions - Wind actions.*
EN. Brussels: CEN, 2005.

6 Appendix

6.1 Dynamic Shear and Moment

The dynamic shear force T_D and the dynamic bending moment M_D at the base of the building are defined in Equations 13a and 13b, respectively. Such that T_s is the static shear force at the base; d is the distance from the base to the section's midpoint [5].

$$T_{Dyn} = T_s C_s C_d \quad (13a)$$

$$M_{Dyn} = T_s d \quad (13b)$$

C_s is the size factor [Equation 14a]; and C_d is the dynamic factor [Equation 14b]. The lack of spatial correlation of wind pressure is considered in C_s where C_d considers the effect of structural vibrations due to wind turbulence when the body enters in resonance mode. Knowing that z_e is the reference height, $l_v(z_e)$ is the turbulence intensity, k_p is the peak factor, B_2 is the background factor, and R_2 is the resonance response factor [5].

$$C_s = \frac{1 + 7 l_v(z_e) \sqrt{B^2}}{1 + 7 l_v(z_e)} \quad (14a)$$

$$C_d = \frac{1 + 2 k_p l_v(z_e) \sqrt{B^2 + R^2}}{1 + 7 l_v(z_e) \sqrt{B^2}} \quad (14b)$$

The reference height is taken to be two thirds of the building's height ($z_e = \frac{2}{3} h = 203.6m$). The turbulence intensity $I_v(z)$ at height z is defined in Equation 15. k_l is the turbulence factor with a recommended value of 1. c_0 is the orography factor which determines the largest increase of the wind velocities occurring near the top of the slope of a hill or cliffs. Since that the slope is zero, $c_0 = 1.0$. z_0 is the roughness length, and it is given a value of 1 for category IV [5].

$$I_v(z) = \frac{\Sigma_v}{v_m(z)} = \frac{k_l}{c_0(z) \ln(z/z_0)} = 0.18 \quad \text{for } z_{min} \leq z \leq z_{max} \quad (15)$$

The background factor which allows the lack of full correlation of the pressure on the structure surface is defined in Equation 16a which is found after solving Equation 16b to find the turbulence length scale at the reference height [5].

$$B^2 = \frac{1}{1 + 0.9 \left(\frac{b+h}{L(z_e)} \right)^{0.63}} = 0.49 \quad (16a)$$

$$L(z_e) = L_t \left(\frac{z_e}{z_t} \right)^{0.67 + 0.05 \ln(z_0)} = 303.6 \quad (16b)$$

The resonance response factor R^2 allows for turbulence in resonance with the considered vibration mode of the structure, and it is defined in Equation 17. Where δ is the logarithmic decrement of damping, approximated to value of 0.05, S_L is the non-dimensional power spectral density function, and R_h and R_b are the aerodynamic admittance functions [5].

$$R^2 = \frac{\pi^2}{2\delta} S_L(z_e, n_{1,x}) R_h(\eta_h) R_b(\eta_b) = 1.77 \quad (17)$$

The non-dimensional power spectral density function in Equation 18 [5].

$$S_L(z_e, n_{1,x}) = 6.8 \frac{f_L(z_e, n_{1,x})}{\left(1 + 10.2 f_L(z_e, n_{1,x})\right)^{\frac{5}{3}}} = 0.13 \quad (18)$$

The non-dimensional frequency $f_L(z_e, n_{1,x})$ is defined in Equation 19 [5].

$$f_L(z_e, n_{1,x}) = n_{1,x} \frac{L(z_e)}{v_m(z_e)} = 0.825 \quad (19)$$

Where v_m is the mean wind velocity at the reference height, which changes for each terrain category. For the terrain category VI, the equation is defined Equation 20 [5].

$$v_m(z_e) = 0.56 v_{ref} \left(\frac{z_e}{10}\right)^{0.3} = 55.2 \text{ m/s} \quad (20)$$

The aerodynamic admittance functions R_h and R_b are defined in Equations 21a and 21b, respectively [5].

$$R_h = \frac{1}{\mu_h} - \frac{1}{2 \eta_h^2} (1 - e^{-2\eta_h h}) = 0.228 \quad (21a)$$

$$R_b = \frac{1}{\mu_b} - \frac{1}{2 \eta_b^2} (1 - e^{-2\eta_b b}) = 0.607 \quad (21b)$$

Such that η_h and η_b are defined in Equations 22a and 22b, respectively [5].

$$\eta_h = \frac{4.6 h}{L(z_e)} f_L(z_e, n_{1,x}) = 3.81 \quad (22a)$$

$$\eta_b = \frac{4.6 b}{L(z_e)} f_L(z_e, n_{1,x}) = 0.862 \quad (22b)$$

The peak factor k_p is the maximum value of the fluctuating part of the response to its standard deviation as shown in Equation 23a. Such that T is the averaging time for mean wind velocity and it can be established at T = 600s, and v is the up-crossing frequency in Hz, which is defined in Equation 23b [5].

$$K_p = \sqrt{2 \ln(v T)} + \frac{0.6}{\sqrt{2 \ln(v T)}} = 3.24 \quad (23a)$$

$$v = n_{1,x} \sqrt{\frac{R^2}{B^2 + R^2}} = 0.13 \quad (23b)$$